Chapter 5

Characterization of Zebrafish Rab5a2

5.1 Introduction.

5.1.1 An introduction to the Rab5 family.

The *rab5* family is the best characterized of all the *rab* families and has been identified as one of the core *rabs* (Bucci et al., 1992; Chavrier et al., 1990). The Rab5 protein localizes to clathrin coated vesicles, early endosomes and the plasma membrane (Bucci et al., 1992). The protein is essential for *in vitro* homotypic fusion of early endosomes and is able to increase the rate of endocytosis *in vivo* when overexpressed (Gorvel et al., 1991; Gruenberg and Howell, 1989; Li and Stahl, 1993). Original experiments done in mammalian cells assumed only one Rab5 and looked at the function of different parts of the protein (Kinsella and Maltese, 1991). Deletion of the entire C-terminal tetrapeptide motif CCSN abolished *rab5* activity but deletion of only the last three residues showed residual *rab5* activity. A mutant containing a 4-residue deletion from the N-terminus retained full activity while N-terminal deletion of 19 residues partially blocked *rab5* activity (Bucci et al., 1992). An amino acid dominant negative Rab5 (N133L) inhibited endogenous Rab5 activity, while a constitutively activate Rab5 (Q79L) had no effect on Rab5 activity (Bucci et al., 1992; Li and Stahl, 1993). In contrast, subsequent studies have shown that overexpression of constitutively active Rab5 causes dramatic enlargement of early endosomes (Stenmark et al., 1994). Overexpression of the wild-type *rab5* enhanced the rate of transferrin receptor internalisation, with *rab5* mutants deficient for GTP binding inhibiting transferrin receptor uptake (Bucci et al., 1992). Taken together these results suggest that Rab5 activity is rate-limiting in the early endocytic pathway. Rab5 has a role in fusion of clathrin-coated vesicles to early endosomes. A cytosolic component containing Rab5-GDI is essential for the Rab5 clathrin-coated pits to sequester transferrin efficiently. Rab5-GDI has been shown to have a role in the earliest stages of the endocytic pathway and is a direct link between the processes of transport vesicle formation and the recruitment of components required for subsequent fusion reactions (Chavrier et al., 1992).

The original Rab5 has now been renamed Rab5a since the discovery of two separate highly similar genes, Rab5b and Rab5c (Singer-Kruger et al., 1994; Wilson and

Wilson, 1992). Interestingly, in the yeast *Saccharomyces cerevisiae*, three highly related Rab5 proteins had already been isolated and named Ypt51p, Ypt52p, Ypt53p (Bucci et al., 1995). These three Rab5s colocalize at the plasma membrane and early endosomes with Rab5b and Rab5c stimulating early endosome fusion *in vitro* and transferrin endocytosis *in vivo*. The ability of Rab5a to regulate transport in the early endocytic pathway is shared by the Rab5b and Rab5c genes with all three proteins being ubiquitously expressed. It has been suggested that the presence of three Rab5 genes may reflect an evolutionary need to ensure Rab5 function even in the presence of a harmful mutation (Chiariello et al., 1999). Alternatively each gene could fulfill a distinct role and be responsible for fine regulation of the early endocytic pathway (Chiariello et al., 1999). The latter hypothesis is supported by recent work showing that all the Rab5 genes are differentially recognized by different kinases. Rab5a is efficiently phosphorylated by extracellular-regulated kinase 1 while cdc2 kinase preferentially phosphorylates Ser-123 of Rab5b. This differential phosphorylation by these kinases could specifically modulate the function of the different Rab5 genes *in vivo* (Christoforidis et al., 1999b).

Rab5 has a large diverse and complex group of interacting molecules, over 20 polypeptides were isolated from bovine brain cytosol that interact both directly or indirectly with the GTP-bound form of Rab5 (Stenmark et al., 1995). The first Rab5 effector identified was Rabaptin-5 which is essential for early endosome fusion (Lippe et al., 2001a; Lippe et al., 2001b). Rabaptin-5 forms a complex with Rabex-5, which catalyses nucleotide exchange on Rab5. When Rab5 is activated by Rabex-5, the Rabaptin-5–Rabex-5 complex induces its own membrane recruitment through Rabaptin-5 (Rybin et al., 1996). This positive-feedback loop counteracts GTP (Lippe et al., 2001a) which is thought to enrich active Rab5 on the membrane, a region where other Rab5 effectors are recruited (Christoforidis and Zerial, 2000; Lippe et al., 2001a; Lippe et al., 2001b). This localized clustering of activated Rab5 proteins is thought to regulate tethering machinery. GTP-bound Rab5 interacts with several other effectors, such as EEA1, Rabenosin5 (Christoforidis and Zerial, 2000), and hVps34 (Nielsen et al., 2000). EEA1 and Rabenosyn5 possess FYVE domains that bind to phosphatidylinositol3phosphate (PtdIns[3]P) (these have been shown also to be Rab5 effectors) (Bucci et al., 1992; Christoforidis et al., 1999b; Stenmark and Aasland, 1999) (Gonzalez-Gaitan et al., 1994). Binding of the FYVE domain to

PtdIns(3)P, complete with interaction of Rab5, is responsible for specific targeting of these proteins to early endosomes.

5.1.2 Rab5 and its role in cell signalling

An important role for Rab5 has been identified in cell signalling. Strigini and Cohen proposed a role for Rab5 in planar transcytosis mediated spread of Wg in the *drosophila* imaginal disc (Strigini and Cohen, 2000) (section 1.2.6.2). However, more recent data using a temperature-sensitive *dynamin* mutant, *shibire,* in *drosophila* which blocks endocytosis suggests Wg spreads extracellularly (Marois et al., 2006). Wg is expressed in a stripe of cells straddling the dorsal-ventral boundary and forms a symmetrical gradient in dorsal and ventral compartments along the imaginal wing disk. When a dominant negative form of Rab5 was expressed in the dorsal compartment, initially Wg protein levels were elevated in dorsal tissue nearest the Wg-expressing cells but, as time progressed, large amounts of Wg invaded the entire dorsal compartment. The authors theorised that this spatial progression of Wg accumulation resulted from intervening tissue no longer internalizing Wg when endocytosis was disrupted. This suggested that Rab5-dependent endocytosis of Wg normally limits the range over which Wg spreads (Marois et al., 2006). In addition, transcription of both *fz2* (a wingless receptor) and *dlp* (a member of the glypicans which have been implicated in the movement of the morphogens Hh, Dpp and Wg) increases, while that of *arrow* (thought to be a wingless co-receptor) decreases rapidly (Marois et al., 2006).

5.1.3 Rab5 genes in zebrafish

There is very little literature on Rabs in zebrafish, with much of this done by Dr Isabel Campos for her PhD thesis (Campos, 2004) and Dr Mathew Clark (Clark, MD, pers. com.). There are two further publications on the zebrafish Rabs and in particular the Rab5 family, from the laboratories of Brand and Heisenberg at Max Planck Institute for Cell Biology (Scholpp and Brand, 2004; Ulrich et al., 2005). Scholpp and Brand (2004) investigated the control of signalling range of Fgf8 by

endocytosis, while Ulrich, Krieg et al. (2005) investigated Rab5c in cell cohesion during gastrulation and the role of Wnt11 (Ulrich et al., 2005).

5.1.3.1 Rab5 in the spread of Fgf8

Scholpp and Brand (2004) report that Rab5s function in endocytosis as regulators of Fgf8 spread. The data showed that Fgf8 colocalises with Rab5 in 54% of vesicles. Injection of a dominant-negative, form of the Fgf receptor XFD decreased internalization of Fgf8 (Amaya et al., 1993). This resulted in an accumulation of the Fgf8 protein around the receiving cells and detection of the Fgf8 protein at greater distances from the source, when compared to uninjected control embryos. When Rab5 function was disrupted by injecting RN-tre (a GAP), Fgf8 was absent from intracellular vesicles and accumulated extracellularly at a greater distance from the source. However, overexpression of Rab5 reduced the range of Fgf8 spreading and increased the size of the Fgf8-positive intracellular compartments. Transplantation experiments showed that when cells injected with RN-tre were transplanted into control embryos near a source of Fgf8, host cells took up the protein, even if cells inhibited for Rab5 function were located between the source and the receiving cells. In these embryos, little extracellular Fgf8 accumulated, unlike embryos where all cells received RN-tre. In embryos where Rab5-overexpressing cells were transplanted, these cells showed an accumulation of Fgf8, while cells that lay behind them were deficient of Fgf8. In embryos injected with RN-tre, expression of Fgf8 target genes *spry4, pea3* and *erm* showed broadened expression compared to controls, knock down of *rab5a2* also showed a broadened expression of *spry4.* Conversely, embryos injected with *rab5a* RNA showed a severe reduction in the induction of *spry4*. This paper has, therefore, suggested a restrictive clearance model for the spread of Fgf8. Endocytosis serves to *restrict* spreading of Fgf8 protein away from the source, by *clearing* Fgf8 protein from the extracellular space via endocytosis, defining how far the protein is able to spread and determining the width of the target tissue responding to Fgf8 signalling. Given that Fgf8 and Rab5 only localizes in a percentrage of cases Scholpp and Brand suggested that the vesicles, which, didn't co-localise with Rab5 might be destined for degradation (Scholpp and Brand, 2004), as Fgf8 was seen in the intracellular degradative pathway of receiving cells. Therefore, they argue that Fgf8 spreads extracellularly by a diffusion-based

mechanism where target cells can actively influence the gradient through endocytosis and subsequent degradation, with the involvement of Fgf receptors (Scholpp and Brand, 2004).

5.1.3.2 Rab5c and its role in cell cohesion

Ulrich, Kreig *et al* (2005) used Rab5 and in, particular, Rab5c's role in endocytosis, to elucidate the effect of Wnt11 on cell cohesion during gastrulation. In particular, the study is concerned with Wnt11's role in controlling prechordal plate progenitor cell movements. Previous work by the authors had shown that prechordal plate in zebrafish is formed by a highly cohesive group of axial mesendodermal progenitor cells which move in a straight path from the germ ring toward the animal pole of the gastrula (Ulrich et al., 2003) and that E-cadherin-mediated cell cohesion is required for the coordinated movement of prechordal plate progenitor cells during zebrafish gastrulation (Montero et al., 2005). Ulrich *et al*. (2005) showed that in wild-type embryos, prechordal plate progenitors moved both toward the overlying epiblast cell layer and along it toward the animal pole. However, embryos lacking *wnt11* (*silberblick* mutants (*slb)*) showed slower movement toward the animal pole with cells often moving in the opposite direction toward the vegetal pole, although cells moved normally towards the epiblast. The coherence of the prechordal plate progenitor cell movements at the onset of gastrulation were also reduced in *slb/wnt11* mutants. The authors suggest that Wnt11 is required to align the movement of individual prechordal plate progenitors and that this alignment might represent a way by which Wnt11 efficiently coordinates prechordal plate progenitor movement toward the animal pole. In addition, the authors suggested that Wnt11 might control alignment of prechordal plate progenitor movement by regulating the cohesion of these cells. In cell cultures, mutant for *wnt11*, large cell aggregates were reduced while small cell aggregates were increased when compared to wild-type. However, when E-cadherin was knocked-down in cultured *wnt11*$^{-/-}$ mutant cells showed no significant differences in aggregates while wild-type cells displayed an increase in small cell aggregates and a decrease in large cell aggregates, compared to wild-type cells with E-cadherin. Wnt11 expression was, therefore, suggested to lead to changes in the subcellular localization of E-cadherin from the plasma membrane into cytoplasmic dots (Ulrich et al., 2005), these dots localized with injected mRNA YFP-

fusion of the zebrafish Rab5c. Wnt11 overexpression was shown to lead to an increase in the proportion of Rab5c-positive endocytic E-cadherin vesicles as did the overexpression of a constitutively active form of *rab5c-YFP* in *slb/wnt11* mutant embryos. *rab5c* MO injected embryos were shown to frequently have a posteriorly displaced and elongated prechordal plate at the end of gastrulation, phenocopying the *slb/wnt11* mutant phenotype. However, *slb/wnt11* mutant embryos, expressing *da-rab5c-YFP*, formed a prechordal plate that was wild-type in appearance, suggesting a rescue of the mutant phenotype. The de-adhesion forces needed to dissociate wild-type versus *slb/wnt11* mutant cells from E-cadherin substrates were decreased, but could be rescued by expressing low amounts of *wnt11* mRNA. Similarly in *rab5c* MO injected cells there was a decrease in the de-adhesion forces when compared to wild type. The study suggests that Wnt11 modulates E-cadherin dynamics through endocytosis and recycling. E-cadherin being partially, but not exclusively, required for Wnt11 control of mesendodermal cell cohesion, suggests a role for other adhesion molecules such as integrins.

5.1.3.3 The zebrafish *rab5*s

Dr Matthew Clark and Dr Isabel Campos have identified 4 zebrafish Rab5s; two Rab5as, Rab5b and Rab5c. Both Rab5as are in the zebrafish online resource zfin (www.zfin.org) - they are termed ‘Rab5a’ and ‘Rab5a like’. In Dr Campos’ thesis these Rabs are re-named Rab5a1 and Rab5a2 respectively (Campos, 2004). Embryos showed no obvious phenotype when *rab5a1* was knocked-down by Dr Campos, however *rab5a2* MO injected embryos showed a very striking gastrulation phenotype, the embryo showed no morphological organizer and died before the completion of epiboly (Figure 5.1.1). In addition, development is drastically slowed when control embryos reach 90% epiboly, compared to *rab5a2* MO injected embryos, which only reach 50% epiboly. In cases where *rab5a2* MO injected embryos reached 80-90% epiboly the blastoderm margin contracted and pinched off the yolk causing its contents to leak and the physiological environment surrounding the blastoderm cells to be disrupted resulting in death (Campos, 2004). *rab5b* MO injected embryos showed thinner and u-shape somites, forebrain defects and cell death in the brain (Campos, 2004). Finally, *rab5c* MO injected embryos showed a similar phenotype to embryos with depleted *rab5b* with u-shape somites, shortened

tail, forebrain defects and cell death in the brain (Campos, 2004). The lack of morphological organizer in the *rab5a2* MO injected embryos led Dr Campos to perform expression analysis for the nodals and their downstream markers. *rab5a2* MO injected embryos displayed a startling lack of expression of the nodals and a majority of their target genes. The MO injected embryos showed no *sqt, cyc, bik, gsc* or *flh* expression and a severe reduction in *ntl* expression compared to control injected embryos (Figure 5.1.2). The dramatic early phenotype seen in *rab5a2* MO injected embryos has, so far, only been seen following the depletion of this Rab, out of all the Rabs screened. Rab5a2's phenotype and the dramatic loss of nodal signalling have led me to further investigate its function and, in particular, its role in nodal signalling.

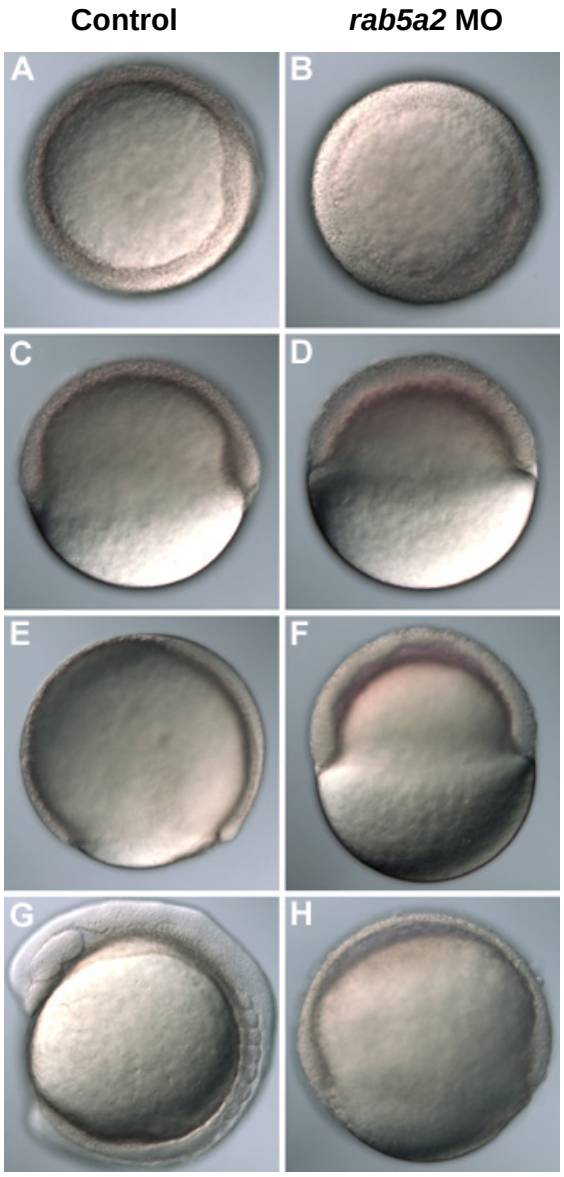

Figure 5.1.1: Time series of 3ng *rab5a2* MO injected embryos (B,D,F,H) compared with control injected embryos (A,C,E,G). Animal view (A) and side view (C) of control injected embryo at shield stage compared to animal view (B) and side view (D) of 3ng *rab5a2* MO injected embryos at the same time point. Control injected embryos at 90% epiboly (E) compared to the same time point in the 3ng *rab5a2* MO injected embryos (F). 8 somite stage control embryo (G) compared to 3ng *rab5a2* MO injected embryo at the same time point (H). (Campos, 2004)

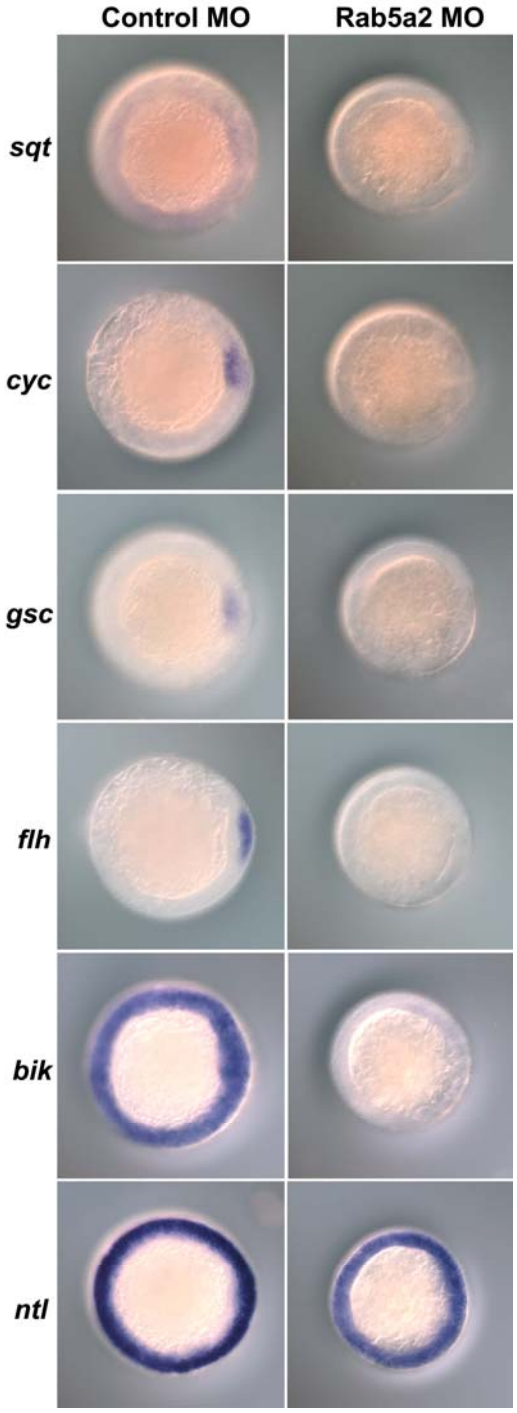

Figure 5.1.2: Comparison of *ish* expression patterns for *sqt, cyc, gsc flh bik* and *ntl* in shield stage control MO injected (left column) and shield stage 3ng *rab5a2* MO injected embryos (right column)(Campos, 2004).

5.2 Reproducibility and further analysis of the Rab5a2 loss of function phenotype.

To characterize Rab5a2, first, it was necessary to check the reproducibility of the loss of function phenotype and the nodal expression pattern seen in the *rab5a2* MO injected embryos. Following this, it was necessary to look more closely at this expression pattern in order to ascertain if there is a temporal element to the expression pattern seen in the *rab5a2* MO injected embryos. In addition it would be interesting to investigate whether the loss of Nodal signalling was due to maternal or zygotic transcripts. Finally, in all other systems that have been studied Rab5a localized to endosomes and has been shown to be responsible for clatherin-mediated endocytosis (Bucci et al., 1995; Bucci et al., 1992; Gorvel et al., 1991). It was therefore important to investigate Rab5a2s effect on other endocytic pathways, and, for this, the role of endocytosis in epiboly was studied.

The *rab5a2* MO injected embryos (*rab5a2* MO injected embryos) are throughout this study compared to 10ng of control MO injected embryos. This control MO is the *rab5a2* MO containing a five base mismatch.

5.2.1 Reproducing the loss of function phenotype

Using the MO designed by Dr Campos, at the dose used in the original investigations, 3ng of *rab5a2* MO was injected and compared to control MO injected embryos. Since the *rab5a2* MO injected embryos showed no phenotype, the dose was increased until an effect was observed. At 5ng of *rab5a2* MO, all embryos died before completing epiboly (n = 47), while at 4ng of MO they all appeared similar to control MO injected embryos (n = 44). When the dose was increased still further to 6ng, the *rab5a2* MO injected embryos died between 30% and 50% epiboly (n = 41/45). In the 5ng *rab5a2* MO injected embryos, at approximately 30% epiboly, fluid appeared to accumulate between the blastoderm cells and the yolk (Figure 5.2.1) this was not seen in control MO injected embryos. In the 6ng *rab5a2* MO injected embryos, this build-up of fluid up, occurred at the earlier stage of approximately 10% epiboly and was more pronounced. In the control MO injected embryos, the cells

appeared as a smooth blastoderm covering the yolk cell, in the *rab5a2* MO injected embryos, the cells appeared to have a substantially rougher blastoderm with cells appearing as a less cohesive group. Finally the *rab5a2* MO injected embryos, as described by Dr Campos, showed substantial developmental delay, compared to control MO injected embryos (Figure 5.2.1).

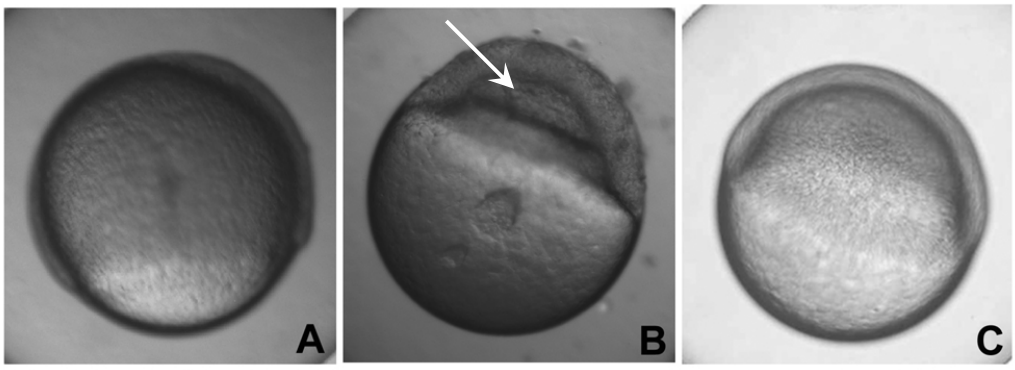

Figure 5.2.1: Control embryo at 70% epiboly (A) compared to 5ng *rab5a2* MO injected embryo at the same time point (B) and control embryo at shield stage (C). Arrow in B indicates the apparent build-up of fluid between the yolk and the cells.

5.2.2 Reproducibility of the expression patterns of nodal and nodal-responsive genes in rab5a2 MO injected embryos.

To reproduce the expression patterns of the nodals and the nodal-responsive genes in the *rab5a2* MO injected embryos, embryos were injected with either 5ng of *rab5a2* MO or 10ng of control MO and fixed at 50% epiboly. The *rab5a2* MO injected embryos showed no expression of the downstream nodal markers *gsc* or *flh* and reduced expression of *ntl* and *bhik.* They also showed no expression of *cyc* (Figure 5.2.2). As with Dr Campos' data, it was difficult to see *sqt* staining in the control embryos, so it is difficult to determine whether *sqt* expression is reduced in the MO injected embryos (Figure 5.2.2). Using a higher dose (6ng) of *rab5a2*, the effect of the MO was to visibly abolish the *bhik* and *ntl* staining in addition to that of *gsc* and *flh.*

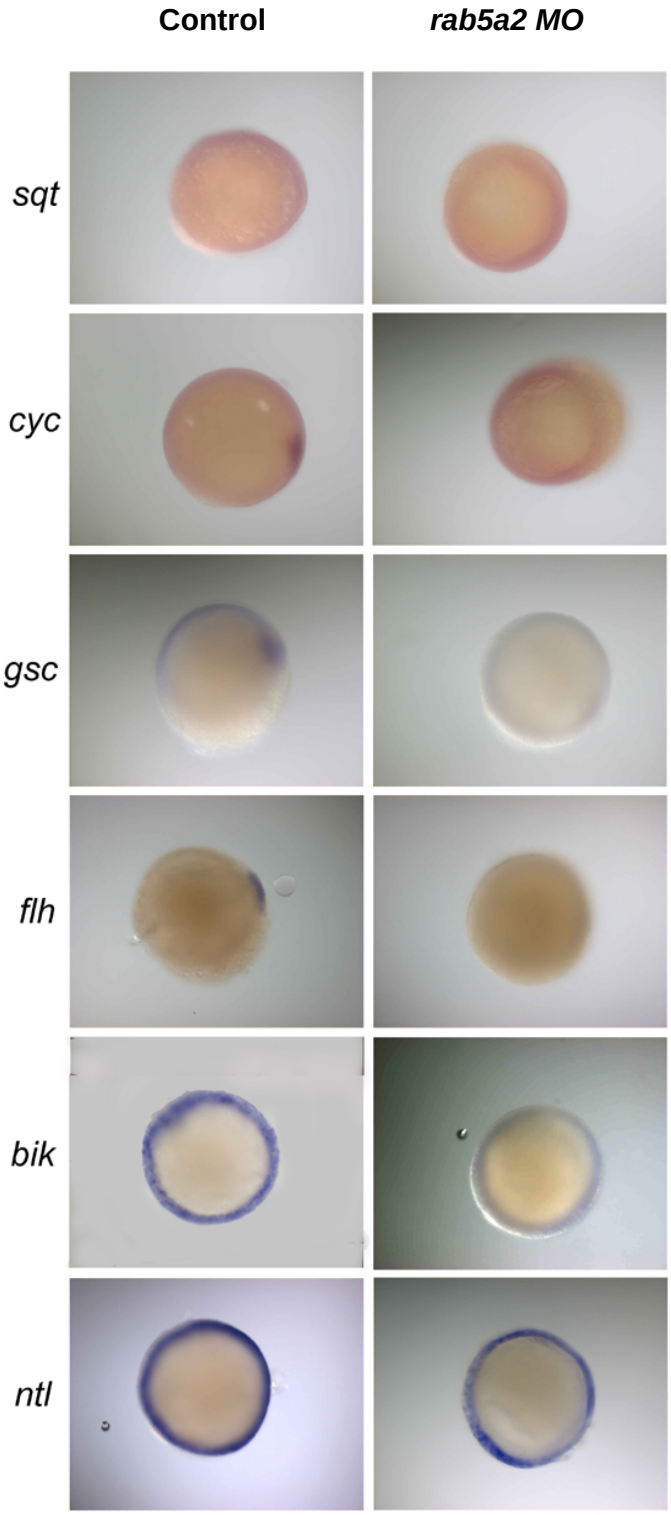

Figure 5.2.2: Animal view of expression patterns of the *nodals* and nodal-responsive genes in shield stage control MO injected and 5ng of *rab5a2* MO injected embryos.

5.2.3 Further analysis of the loss of function phenotype

To establish whether the loss of nodal signalling is time and dose dependent, embryos were injected with either 2ng, 5ng or 8ng of *rab5a2* MO and along with 10ng control morpholino injected embryos were fixed at four time points (30%, 50%, 70% and 90% epiboly). Subsequently, expression patterns of *gsc* and *ntl* were examined. These two genes are induced by differing doses of nodal so should provide an accurate picture of Nodal signalling at these time points. Furthermore, the expression pattern of the dorsal marker *chordin* was recorded, to investigate if nodal signalling alone was affected, or whether the effect relates to the establishment of dorsal in general.

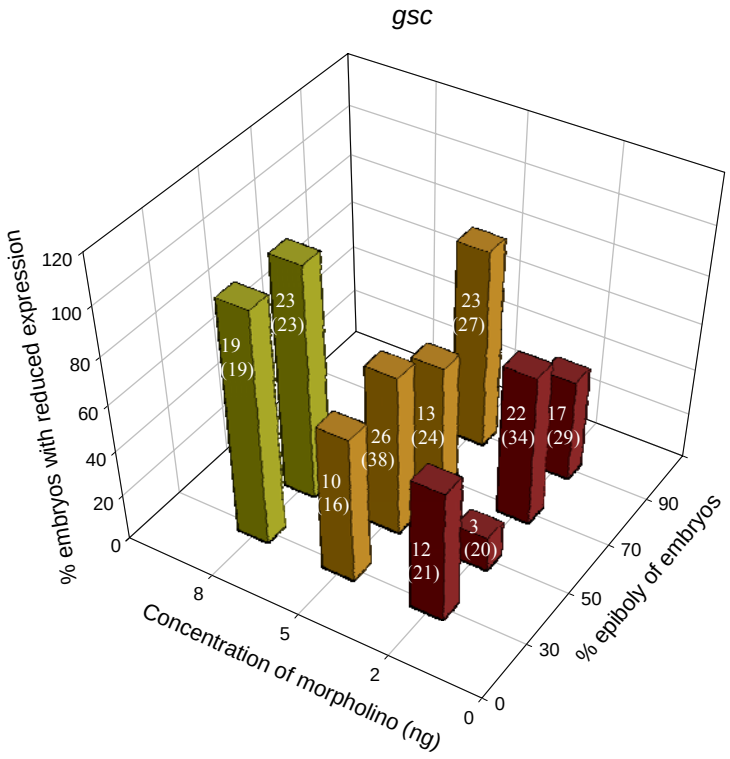

Figure 5.2.3: Graph showing the percentage of embryos that showed a reduction in expression of *gsc* at either 2ng, 5ng or 8ng of *rab5a2* MO and at 30%, 50%, 70% and 90% epiboly stages.

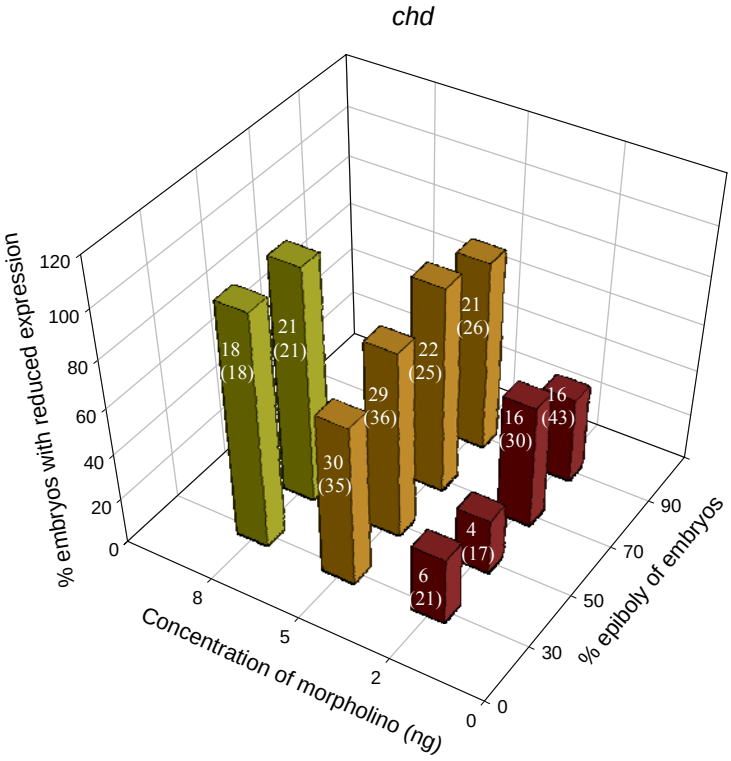

Figure 5.2.4: Graph showing the percentage of embryos that showed a reduction in expression of *chd* at either 2ng, 5ng or 8ng of *rab5a2* MO and at 30%, 50%, 70% and 90% epiboly stages.

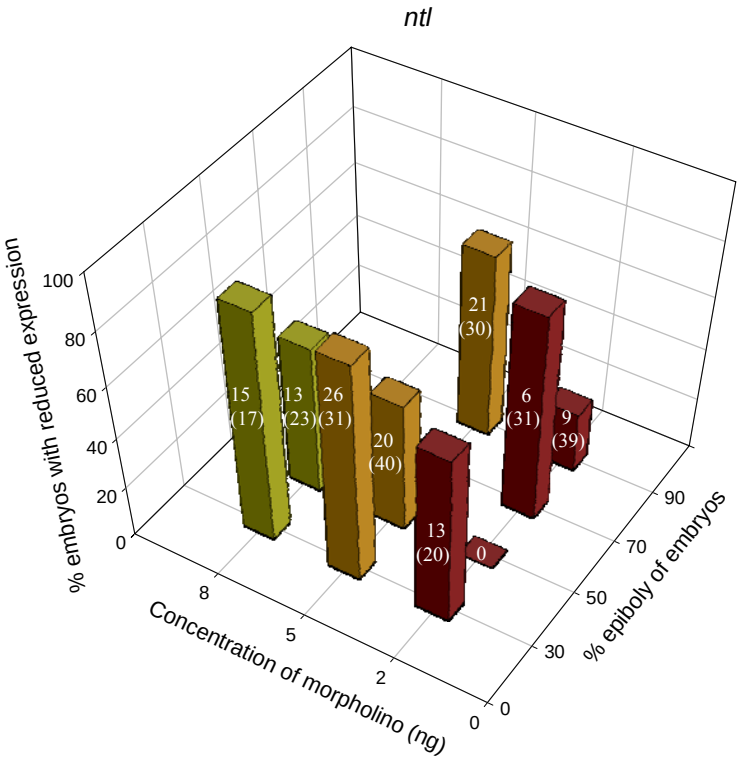

Figure 5.2.5: Graph showing the percentage of embryos that showed a reduction in expression of *ntl* at either 2ng, 5ng or 8ng of *rab5a2* MO and at 30%, 50%, 70% and 90% epiboly stages.

The expression of *gsc* in the 2ng MO injected embryos was reduced in 45-65% of the embryos between 30-90% epiboly. However the number of embryos showing a reduction in *gsc* expression fell to only 15% at 50% epiboly (Figure 5.2.3). Increasing the dose of MO to 5ng resulted in between 55-85% of the embryos showing a reduction in *gsc* expression between 30-90% epiboly (Figure 5.2.3). At the highest dose of morpholino all the 30% and 50% epiboly embryos showed a decrease in *gsc*, however, by 70% epiboly all the 8ng embryos were dead (Figure 5.2.3).

The expression of *ntl* in all the *rab5a2* MO injected embryos was variable. The 2ng MO injected embryos showed a reduction in *ntl* expression of 65% at 30% epiboly. At 50% epiboly no embryos showed an obvious reduction in *ntl* expression, at 70% 79% of embryos showed reduced expression while at 90% epiboly only 23% of embryos showed a reduction in *ntl* expression (Figure 5.2.5). Increasing the dose to 5ng resulted in between 50-85% of embryos showing a reduction in *ntl* expression between 30-90% epiboly. However, at 50% epiboly the number of embryos that showed reduced *ntl* expression had fallen to just 3% (Figure 5.2.5). Increasing the dose still further resulted in 88% and 57% of the embryos showing reduced expression of *ntl* at 30% and 50% epiboly respectively. At 70% and 90% all the 8ng *rab5a2* MO injected embryos had died (Figure 5.2.5).

The expression of *chd* in the 2ng *rab5a2* MO injected embryos was reduced in between 25-50% of the embryos between 30-90% epiboly (Figure 5.2.4). When the dose of the MO was increased to 5ng between 70-90% of the MO injected embryos showed a reduction in *chd* expression at between 30-90% epiboly (Figure 5.2.4). When the dose of *rab5a2* MO was increased still further all of the embryos showed a reduction in *chd* expression at 50% and 30% epiboly stages. However at 70% epiboly and 90% epiboly all the embryos had died (Figure 5.2.4).

5.2.4 Maternal verses zygotic

The early phenotype of the *rab5a2* MO injected embryos and the ubiquitous expression pattern of *rab5a2* seen as early as the one cell stage (zfin) suggests that maternal *rab5a2* plays an important role in zebrafish development. In order to ascertain whether this is the case a splice MO was designed, this straddles a splice site of the gene of interest and so binds, in part, to the intronic and, in part, to the exonic section of the gene. This ensures that the MO only binds to transcripts that have not yet been spliced, such as zygotic transcripts (Draper et al., 2001).

Embryos were injected with either 10ng of *rab5a2* splice MO or 10ng of control MO. At shield stage the *rab5a2* splice MO injected embryos were comparable to controls showing a visible organizer unlike the *rab5a2* morpholino injected embryos. However by 24hpf the *rab5a2* splice MO injected embryos appeared as an accumulation of dead cells on top of the yolk (Figure 5.2.6).

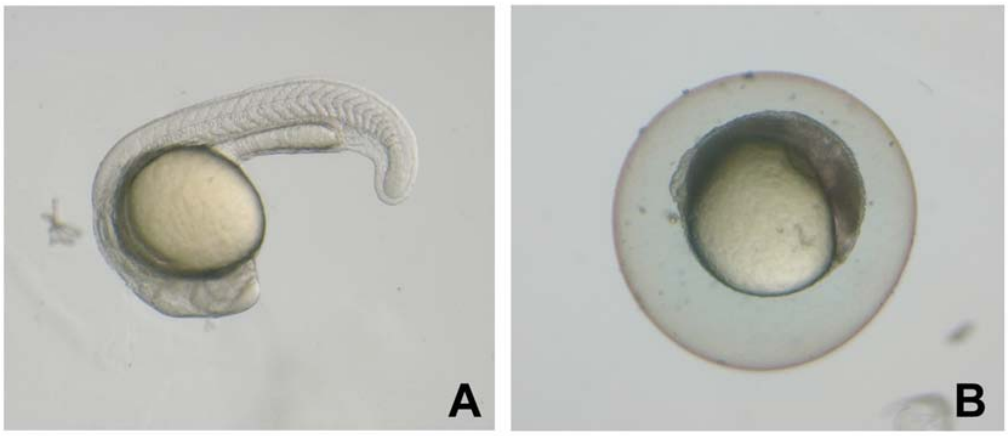

Figure 5.2.6: Lateral view of 24hpf embryos: control MO injected embryo (A) compared to 8ng *rab5a2* splice MO injected embryo (B).

Although the *rab5a2* splice MO injected embryos had showed massive cell death at 24hpf at shield stage they had a visible organizer, it was therefore necessary to look at the expression pattern of the nodal responsive genes *ntl, bik* and *gsc* and the dorsal marker *chd.* The *rab5a2* splice MO injected embryos and control MO injected

embryos were fixed at 50% epiboly. Analysis of the expression patterns for *gsc*, *ntl* and *chd* in the splice MO injected embryos showed them to be similar to those seen in the controls (Figure 5.2.7). *bik* expression however appeared slightly reduced in the splice MO injected embryos (n = 10/12).

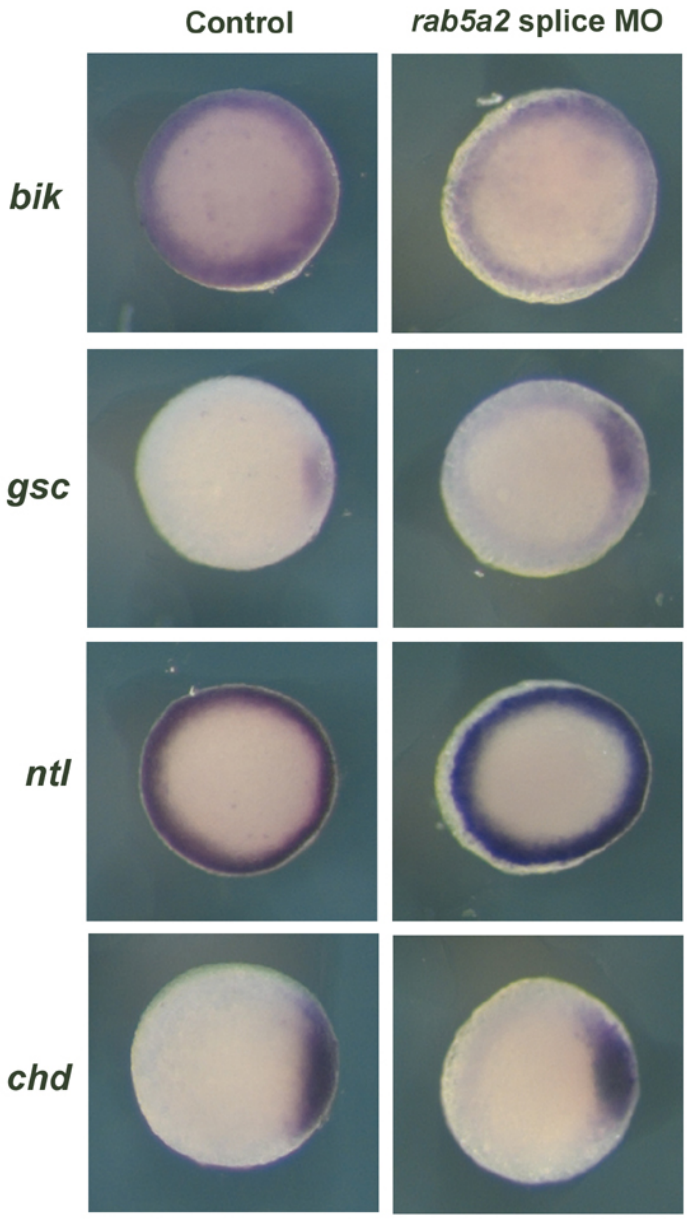

Figure 5.2.7: Animal views of shield stage embryos*: gsc, ntl, chd* and *bik* expression in control MO injected embryos on the left compared to 10ng *rab5a2* splice MO injected embryos on the right

5.2.5 The effect of loss of Rab5a2 function on epiboly movements

Epiboly in zebrafish is considered, in part, an endocytic event (Betchaku and Trinkaus, 1986). Therefore, to ascertain whether the phenotype seen in *rab5a2* MO injected embryos is, in some part, due to its effect on the role of endocytosis during epiboly, the epiboly movements of *rab5a2* MO injected embryos were compared with those of controls, at three different time points of epiboly. The embryos were placed in 1x Danieau solution, containing 5mg/ml biotinylated dextran (10,000mw), at dome stage (start of epiboly), 30% epiboly and shield stage for 15 minutes, they were then washed three times in 1x Danieau solution and immediately fixed in 4% PFA. Once fixed, the embryos were stained for biotin (Solnica-Krezel et al., 1994). The control MO injected embryos, at dome stage and 30% epiboly, all showed a ring of staining around the leading edge of the blastoderm (Figure 5.2.8). At shield stage, this staining formed more of a gradient moving from the dorsal to ventral side of the embryo. The *rab5a2* MO injected embryos showed very little staining at dome stage (n = 13/17) and even less staining at 30% (n = 12/13). There was no staining seen in the *rab5a2* MO injected embryos at shield stage (n = 14/15) (Figure 5.2.8).

The *rab5a2* MO injected embryos showed defects in endocytosis however epiboly did proceed but at a slower pace and did not complete. This suggested that the microtubules in the yolk were unaffected and were responsible for epiboly proceeding as far as it did. Cold shock depolarizes microtubules therefore 5ng *rab5a2* MO injected embryos and control MO injected embryos were placed at 20°C and monitored overnight. The control embryos developed normally (n =16/16) but with some developmental delay whereas the *rab5a2* MO injected embryos arrested and died at sphere stage to very early epiboly (n = 14/14) (Figure 5.2.9, supplemental movie 5.2.9). The *rab5a2* MO injected siblings that were incubated at 28°C died at the later stage of 70% epiboly while the control MO injected siblings incubated at 28°C developed normally.

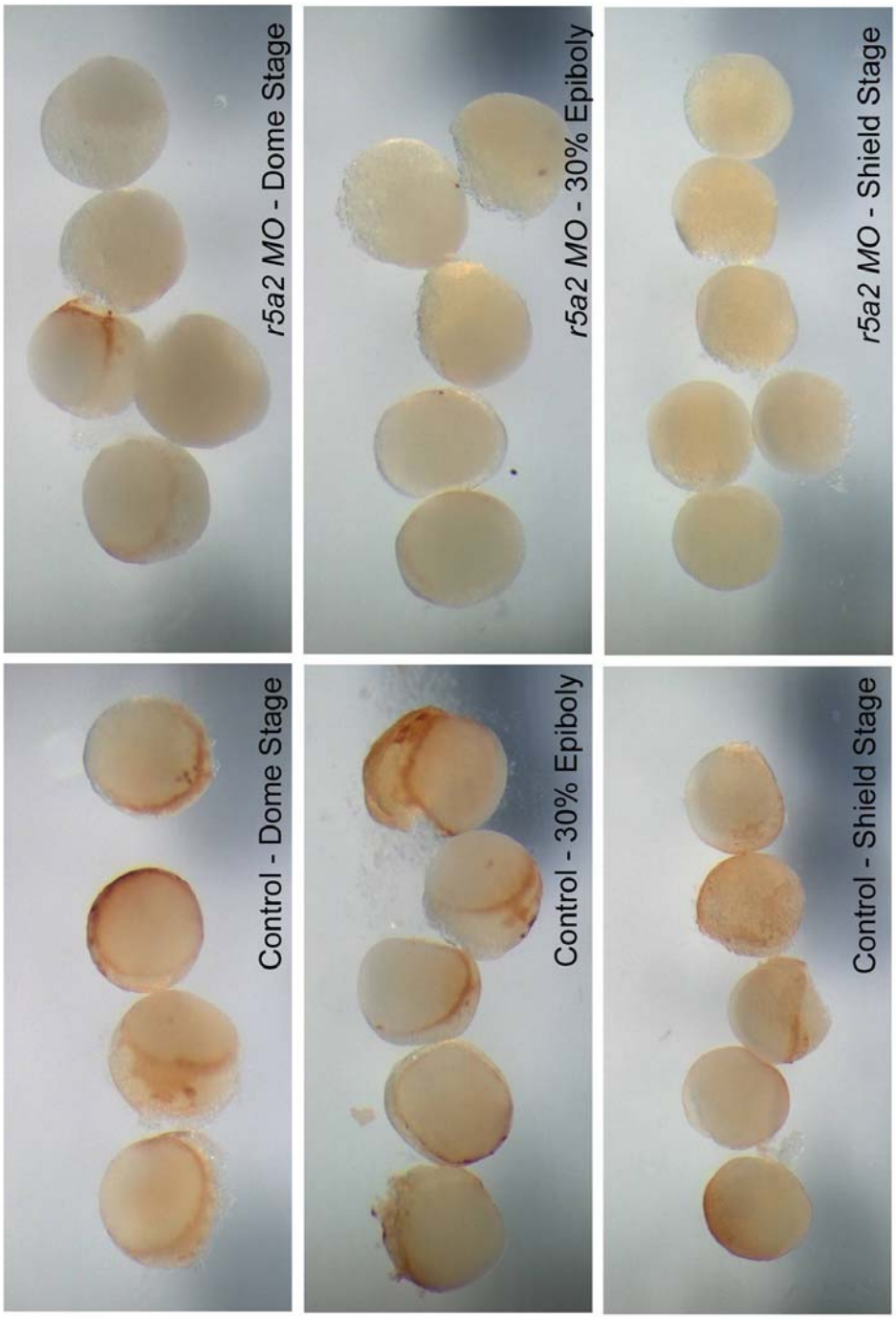

Figure 5.2.8: The right column shows the effect of 5ng of *rab5a2* on different stages of epiboly when compared with control MO injected embryos in the left column.

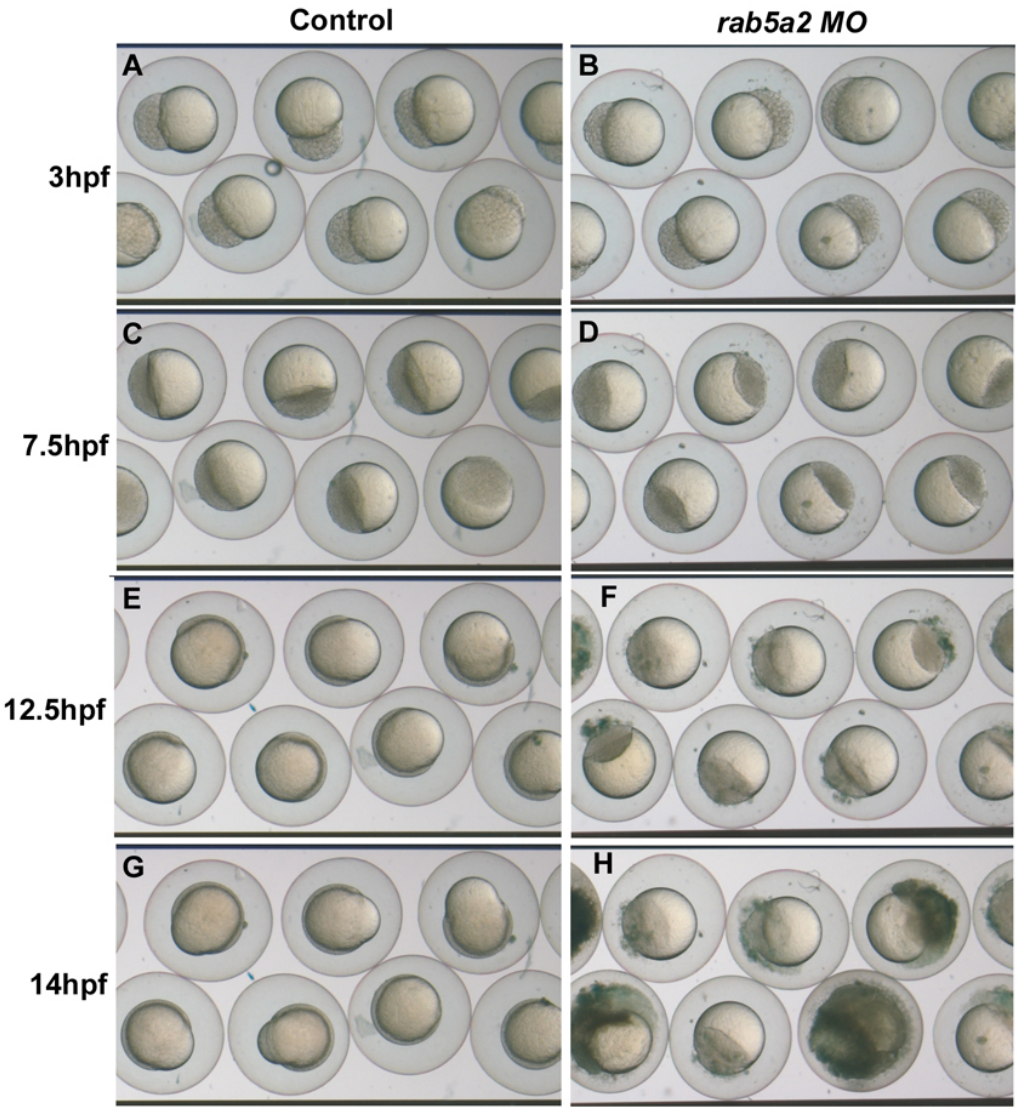

Figure 5.2.9: A time series of embryos cold shocked at 20°C: 3hpf control MO injected embryos (A) compared to *rab5a2* MO injected embryos (B). 7.5hpf control MO injected embryos (C) compared to *rab5a2* MO injected embryos (D). 12.5hpf control MO injected embryos (E) compared to *rab5a2* MO injected embryos (F). 14hpf control MO injected embryos (G) compared to *rab5a2* MO injected embryos (H).

5.3 Analysis of overexpression of Rab5a2

5.3.1 Rab5a2 overexpression

Wild type *rab5a2* mRNA was overexpressed in wild type embryos by injecting 1.5ng of *rab5a2* capped mRNA. At 40-50% epiboly, an accumulation of cells became apparent on the animal pole of approximately one third of the *rab5a2* overexpressing embryos (n = 14/41). In the remaining *rab5a2* overexpressing embryos, the organiser appeared larger (n = 27/41), when compared with MO buffer injected embryos (Figure 5.3.1). The *rab5a2* overexpressing embryos then appeared to arrest for approximately one hour, during which time either the accumulation of cells on the animal pole disappeared, or the enlarged organiser reduced in size and the embryo became what appeared phenotypically wild type (n = 41/41). At 24hpf, approximately two thirds of the *rab5a2* overexpressing embryos appeared similar to MO buffer injected embryos, except for an enlarged yolk extension (n = 27/39). The remaining third had a reduced body axis and reduced head size (n = 12/39). By 5dpf, all the *rab5a2* overexpressing embryos show a severely shortened body axis and thicker, less extended yolks (n = 38/38), compared to MO buffer injected embryos (Figure 5.3.1).

5.3.2 Nodal markers expression pattern in Rab5a2 overexpressing embryos

To establish whether overexpression of *rab5a2* affected the expression pattern of nodal markers, embryos were fixed at shield stage and stained for *bik*, *ntl, gsc* and *chd* expression by *in situ hybridization*. In both the MO buffer injected embryos and the *rab5a2* overexpressing embryos, the *bik* expression patterns were similar (Figure 5.3.2). A similar expression pattern between MO buffer injected embryos and *rab5a2* overexpressing embryos was also seen for *ntl.* There appeared to be a small difference in the expression pattern of *chd*, with the *rab5a2* overexpressing embryos showing *chd* expression encroaching into the ventral region more than in MO buffer injected embryos (Figure 5.3.2). There was a substantial difference in *gsc* expression pattern between the MO buffer injected embryos and the *rab5a2* overexpressing

embryos. The *rab5a2* overexpressing embryos showed the same *gsc* expression pattern as the MO buffer injected embryos on the dorsal side of the embryo but in addition there was *gsc* expression on the animal pole closest to the ventral side of the embryo (Figure 5.3.2). This expression was not seen in the MO buffer injected embryo (Figure 5.3.2) and was stronger than the dorsal expression seen in these embryos.

To further analyse this result, *rab5a2* overexpressing embryos and MO buffer injected embryos were fixed at 30%, 50%, 70% and 90% epiboly so that the expression pattern of *chd, ntl* and *gsc* could be followed over time. At 30% epiboly, the *rab5a2* overexpressing embryo showed expression of *gsc* in the ventral region, in addition to its usual dorsal expression. This additional expression pattern was seen in 83% of the embryos (n = 10/12). Interestingly, at this stage *ntl* expression in the *rab5a2* overexpressing embryos shows spots of staining in the animal pole, compared to the marginal expression observed in the MO buffer injected embryos. This expression of *ntl* was seen strongly in 50% (n = 6/12) of the *rab5a2* overexpressing embryos, with a further 17% exhibiting weaker staining (n = 2/12) (Figure 5.3.3). At 50% epiboly 73% of the *rab5a2* overexpressing embryos (n = 8/11) show strong additional staining in the animal pole of embryos stained for *gsc* expression, while 18% of the experimental embryos showed fainter (n = 2/11), additional *gsc* staining. At this stage, most of the embryos, stained for *ntl* expression, showed no additional staining (n = 11/12). However 67% of *rab5a2* RNA injected embryos (n = 8/12) showed *ntl* staining which began to encroach on the animal pole from its marginal domain, showing a thicker band of staining round the embryo than is seen in MO buffer injected embryo (Figure 5.3.3).

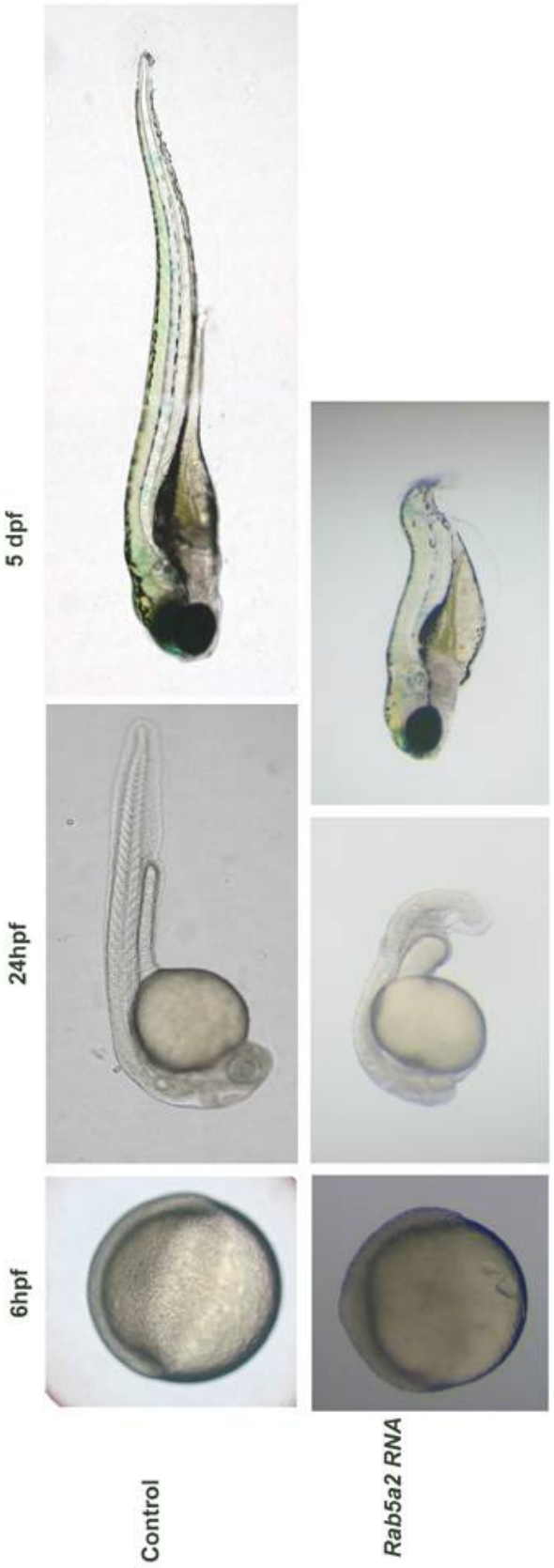

Figure 5.3.1: A shield stage 1.5ng *rab5a2* overexpressing embryo compared to shield stage MO buffer injected embryo. Lateral view of 24hpf 1.5ng *rab5a2* overexpressing embryo compared to 24hpf MO buffer injected embryo. Lateral view of 5dpf 1.5ng *rab5a2* overexpressing embryo compared to 48hpf MO buffer injected embryo

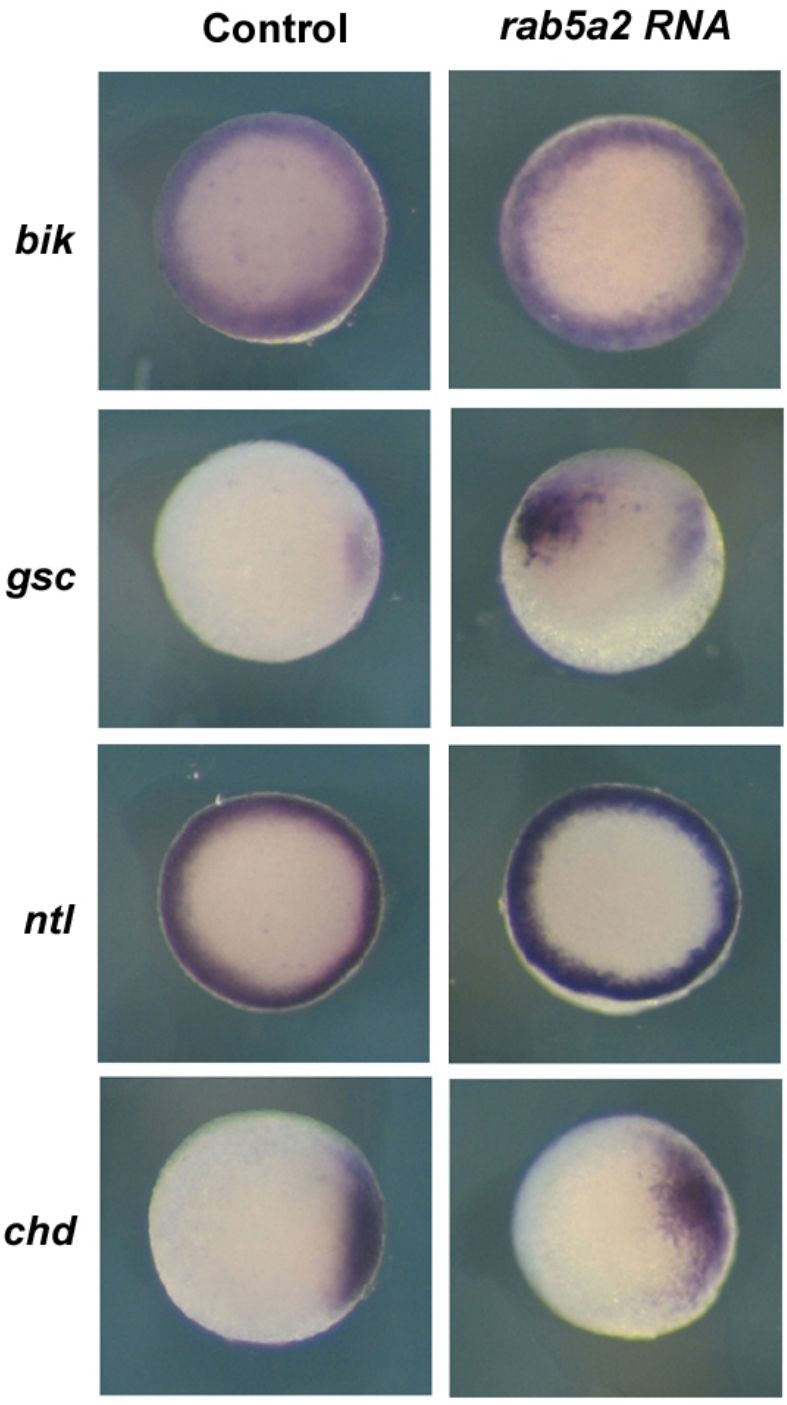

Figure 5.3.2: Animal view of expression patterns of the nodal and dorsal markers in control injected and *rab5a2* overexpression embryos at shield stage.

At 70% epiboly, 39% of *rab5a2* RNA injected embryos show strong additional *gsc* expression in the animal pole (n = 5/13), while 23% show weak additional *gsc* expression (n = 3/13) when compared to MO buffer injected embryos (Figure 5.3.3). *ntl* expression at this stage in *rab5a2* RNA injected embryos is seen in the margin comparable with MO buffer injected embryos. In addition, there is strong staining in the animal pole in 39% of the experimental embryos (n = 5/13), with similar but weaker staining seen in another 31% of experimental embryos (n = 4/13) (Figure 5.3.3). The 90% epiboly *rab5a2* RNA injected embryos continue to show mislocalized expression of both *gsc* and *ntl* with additional staining when compared to MO buffer injected embryos (Figure 5.3.3). At this stage, the number of embryos that have this unusual *gsc* staining has fallen to 50% (n = 5/10) while those that have the strong unusual *ntl* staining remains at around 70% (n = 7/10). The *chd* expression pattern is unchanged in experimental embryos, compared to the MO buffer injected embryos in 30% (n = 12), 50% (n = 11), 70% (n = 10) and 90% (n = 10) epiboly. However, the strength of this expression appears stronger in *rab5a2* RNA injected embryos compared to MO buffer injected embryos at the 70% (n = 10/10) and 90% (n = 10/10) epiboly stages (Figure 5.3.3).

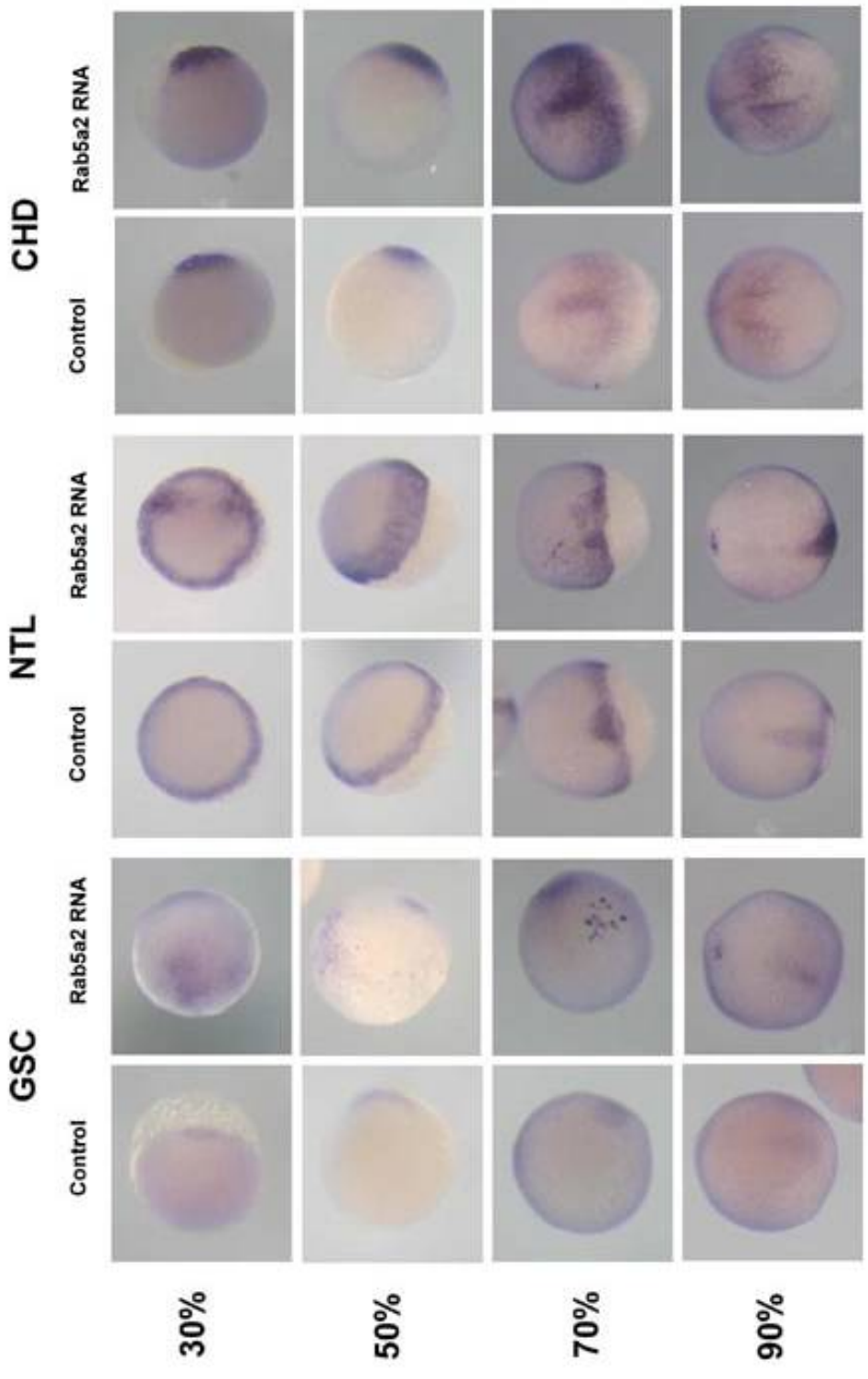

Figure 5.3.3: Showing the expression patterns of *gsc*, *ntl* and *chd* in control and Rab5a2 overexpressing embryos at 30%, 50%, 70% and 90% epiboly. *gsc* expressing embryos are shown as animal pole views as are 30% epiboly *ntl* expressing embryos and 30% and 50% *chd* expressing embryos. The remainder of the embryos are shown as a side view for improved visualisation of expression patterns

5.3.3 The effect of constitutively active Rab5a2 on the zebrafish embryo

Much of the experimental work described in the literature describes the use of a constitutively active version of Rab5 for overexpression experiments. One base change in the injected RNA ensures that the Rab is locked in its GTP-bound form and so constantly active. The dose of wild-type *rab5a2* RNA, needed to elucidate an overexpression phenotype was high; this is due to the many regulators of Rab function found *in vivo* eg. GAP, GDI etc. In order to overexpress wild type Rab protein, these regulators must be overcome by superior numbers of Rab protein. However, injection of constitutively active *rab5a2* RNA (da-*rab5a2* RNA) would not require such a large dose of RNA as it is locked in the GTP-bound form and, therefore, would be little affected by regulatory factors. Embryos injected with increasing doses of the *da-rab5a2* RNA were examined.

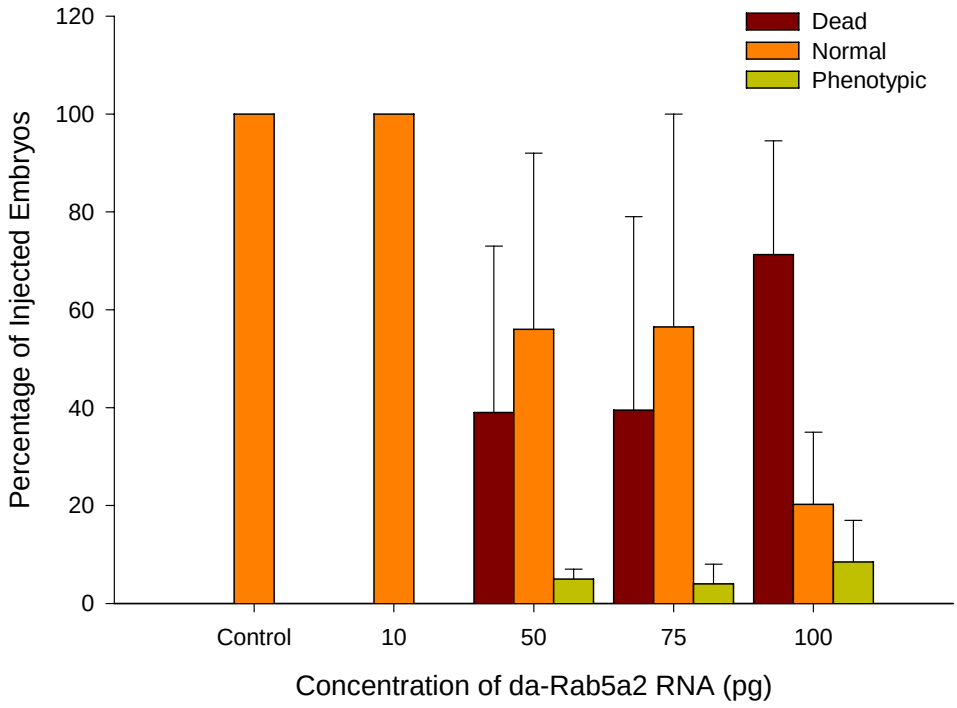

Figure 5.3.4: Comparison of different doses of *da-rab5a2* RNA and the effect it has on 24hpf embryos.

Injection of 10pg of constitutively active *rab5a2* RNA resulted in no phenotype being observed (n = 10/10, n2 = 28/28) and the embryos were comparable with MO buffer injected embryos (n = 51/51) (Figure 5.3.4). Injection of 50pg of *da-rab5a2* RNA showed a small percentage of embryos with a phenotype similar to that seen in wild-type *rab5a2* RNA injected embryos (n1 = 1/39, n2 = 1/15), however, approximately 39% died (n1 = 2/39, n2 = 11/15), while the remainder looked normal (n1 = 36/39, n2 = 3/15). When the dose of *da-rab5a2* RNA was increased to 75pg, again, only a small percentage, approximately 4% (n1 = 7/85, n2 = 0/19), showed a phenotype similar to the wild type *rab5a2* RNA overexpression, while 40% of the *da-rab5a2* overexpressing embryos died (n1 = 67/85, n2 = 0/19). At 100pg over 70% of the da-*rab5a2* RNA injected embryos died (n1 = 86/91, n2 = 11/23), with only 8% showing a wild type *rab5a2* RNA overexpression phenotype (n1 = 0/91, n2 = 4/23) (Figure 5.3.4). Although the percentage of embryos showing a phenotype seemed to increase in relation to the percentage of normal embryos, the actual number that survived became smaller. This reduction in viable embryo numbers, coupled with the fact that constitutively active *rab* RNA has been artificially modified, resulted in the decision not to use this *da-rab5a2* RNA for further studies but to use the wild type *rab5a2* RNA.

5.4 The effect of Rab5a2 on exogenous Nodal signalling

Examining the effect of Rab5a2 on exogenous nodal signalling enables the events that induce nodal signalling in the developing embryo to be separated from those that transport the nodal signal. Squint has been proposed as a morphogen (Chen and Schier 2001) acting directly on target cells over a distance while Cyclops signals in a more localized manner, because of these difference in signalling action it is important to look at both of these nodal proteins. To examine the role of exogenous nodal signalling, RNA encoding either *sqt* or *cyc* was injected, along with the lineage label biotinylated-dextran into a single cell at the centre of the animal pole of embryos at the 128 cell stage. These embryos were allowed to develop for three hours and then fixed for *ntl* and *gsc* expression analysis. The daughter cells of the original injected cell will all produce the nodal signal derived from the RNA with which the original cell was injected. These daughter cells will also stain for biotinylated-dextran allowing accurate visualisation of those cells producing the nodal signal. Injection into the middle of the animal pole avoids the exogenous produced *gsc* or *ntl* expression from encroaching on the area of the embryo where endogenous expression of *gsc* or *ntl* is evident. These single cell injections were performed into embryos injected at the one cell stage with either a control MO, 5ng of *rab5a2* MO or 1.5ng of *rab5a2* RNA.

5.4.1 Injection of 5pg of squint into a single cell of 128 cell stage embryo

Control MO injected embryos showed *gsc* expression close to the cells producing Sqt (Figure 5.4.1) (n = 15/19) with possible faint expression in an additional three embryos (n = 3/19). The *rab5a2* MO injected embryos showed a considerably fainter but broader band of *gsc* expression (n = 8/10) (Figure 5.4.1). In embryos overexpressing *rab5a2 gsc* expression was similar to that seen in control embryos (n = 6/12) with faint expression in an additional four embryos (Figure 5.4.1). Control MO injected embryos showed expression of *ntl* in a broad ring around the Sqt

producing cells (n = 25/25) (Figure 5.4.1). The *rab5a2* MO injected embryos showed reduced intensity of expression of *ntl* (n = 4/14), whilst there was very faint possible expression in an additional seven embryos (Figure 5.4.1). In embryos overexpressing Rab5a2, there was strong *ntl* expression, similar to that seen in control embryos (n=7/8) (Figure 5.4.1).

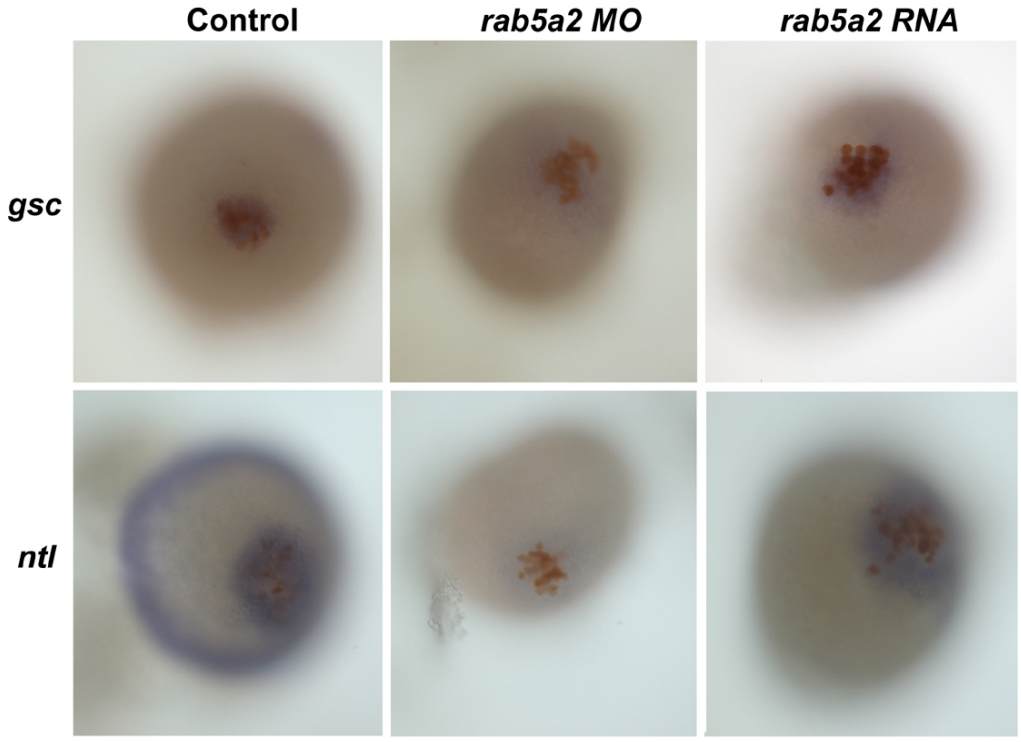

Figure 5.4.1: Showing the expression of *gsc* and *ntl* in control, *rab5a2* MO and *rab5a2* RNA injected embryos when 5pg of *sqt* RNA are injected into the animal pole of 128 cell stage embryos (where blue is *gsc* or *ntl* expression and brown the cells injected with *sqt* RNA).

5.4.2 Injection of 10pg of squint into a single cell of 128 cell stage embryo

Control injected embryos showed exogenous *gsc* expression close to the cells producing the Sqt signal (n = 7/11) (Figure 5.4.2) with reduced expression in the remainder. *ntl* expression in the control embryos was seen as a thick band surrounding the Sqt producing cells (n = 7/8) with reduced expression in the remaining embryo. The *rab5a2* MO injected embryos showed a broad band of faint *gsc* expression (n = 3/12), while some embryos showed very faint staining (n =2/12).

However, over half of the embryos showed no *gsc* expression (n = 7/12). The *rab5a2* MO injected embryos showed faint *ntl* expression (n = 5/21) an additional eight embryos showed very faint to no expression whilst the remaining eight showed no staining (Figure 5.4.2). Exogenous *gsc* expression in *rab5a2* overexpressing cells was comparable to control exogenous expression of *gsc* in (n =10/13). The remaining three embryos showed no *gsc* expression. Exogenous expression of *ntl* in the *rab5a2* overexpressing embryos showed expression comparable to controls (n = 12/21) with reduced expression in an additional seven embryos. The remaining embryos showed no *ntl* expression (Figure 5.4.2).

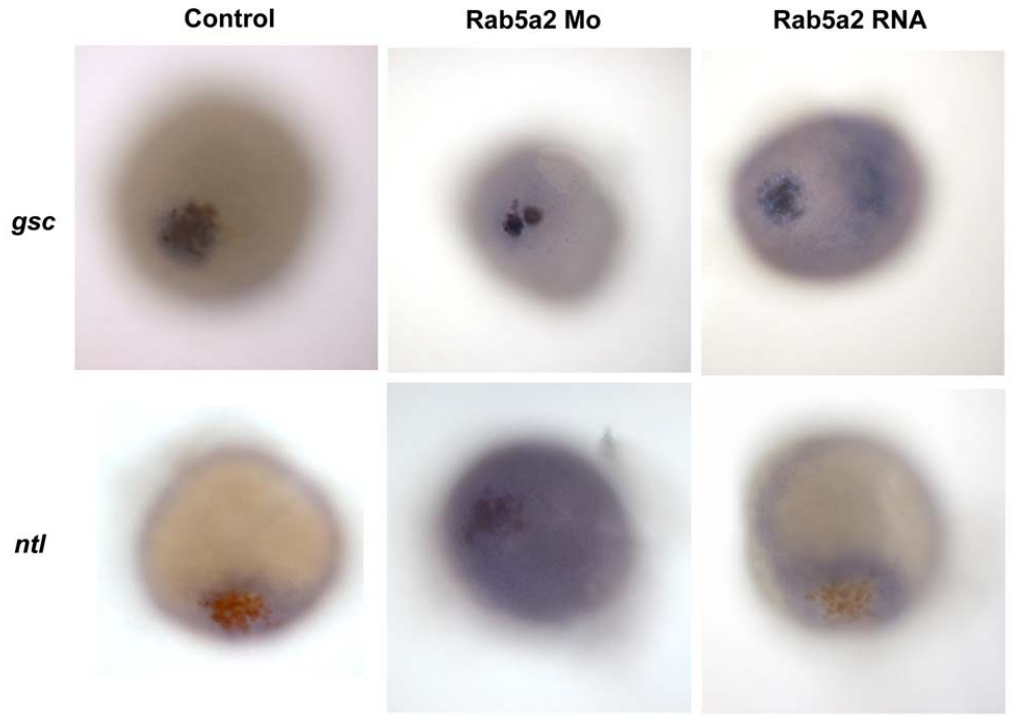

Figure 5.4.2: Showing the expression of *gsc* and *ntl* in control, *rab5a2* MO and *rab5a2* RNA injected embryos when 10pg of *sqt* RNA are injected into the animal pole of 128 cell stage embryos (where blue is *gsc* or *ntl* expression and brown the cells injected with *sqt* RNA).

5.4.3 Injection of 7pg of cyclops into a single cell of 128 cell stage embryo

Control MO injected embryos showed *gsc* expression close to the cells producing Cyclops (n = 7/10) (Figure 5.4.3) with fainter staining in an additional three embryos. The *rab5a2* MO injected embryos showed a fainter expression of *gsc* than in controls (n = 6/19), with the remainder showing no staining (n = 13/19). *rab5a2* overexpressing embryos showed no expression of *gsc* in half of the embryos (n = 6/12), three embryos showed expression comparable to controls while the last three showed faint expression (Figure 5.4.3). Control injected embryos showed a band of *ntl* expression thinly round the Cyclops producing cells (n = 8/9). *rab5a2* MO injected embryos showed no *ntl* expression in nearly half the embryos (n = 7/15) while four showed possible very faint staining and the remainder showed *ntl* expression comparable with controls. The *rab5a2* overexpressing embryos showed *ntl* expression comparable to controls in the majority of embryos (n = 10/14) with the remaining four showing no visible *ntl* expression (Figure 5.4.3).

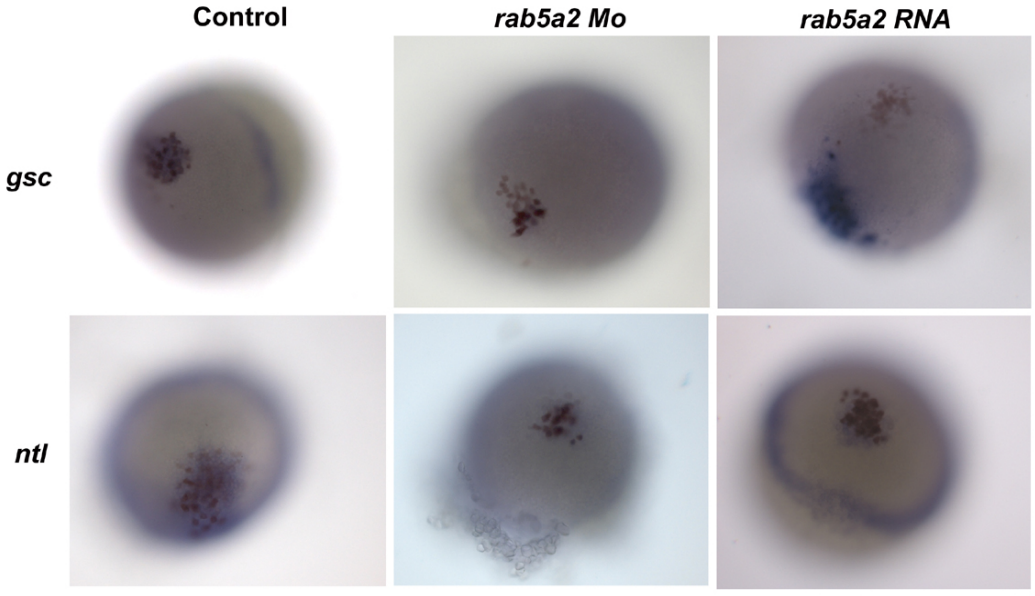

Figure 5.4.3: Showing the expression of *gsc* and *ntl* in control, *rab5a2* MO and *rab5a2* RNA injected embryos when 7pg of *cyc* RNA are injected into the animal pole of 128 cell stage embryos (where blue is *gsc* or *ntl* expression and brown the cells injected with *cyc* RNA).

5.5 Additional functions for Rab5a2 in the developing embryo

5.5.1 The contribution of Rab5a2 in the YSL

A source of many patterning and signalling factors, including Nodal is the YSL; it was, therefore important to ascertain whether Rab5a2 plays a role in the YSL. In order to achieve this, *rab5a2* MO was injected into the yolk cell of 1000 cell stage embryos. Injection into the yolk at this stage is thought to ensures that the MO only has an effect in the yolk as the cells of the embryo after the four cell stage no longer enable free movement of RNA between cells (Hsu et al., 2006).At 24hpf the *rab5a2* MO injected embryos showed slightly curved tails compared to control. By 48hpf, the *rab5a2* MO injected embryos looked dramatically different from controls; retaining the curved tails seen at 24hpf they now showed a thinner axis with reduced pigment (Figure 5.5.1 B) when compared to controls (Figure 5.5.1 A). Most dramatically though, the *rab5a2* MO injected embryos showed an accumulation of what appeared to be dead cells on the part of the yolk attached to the embryo. This section of the embryos in controls is the site of the developing heart with blood being observed on the dorsal part of the yolk (Figure 5.5.1 C). In addition, this section will give rise to organs such as the gut kidney and liver. In the *rab5a2* MO injected embryos there is no apparent heart (Figure 5.5.1 D and E) and the embryos die at approximately 3dpf.

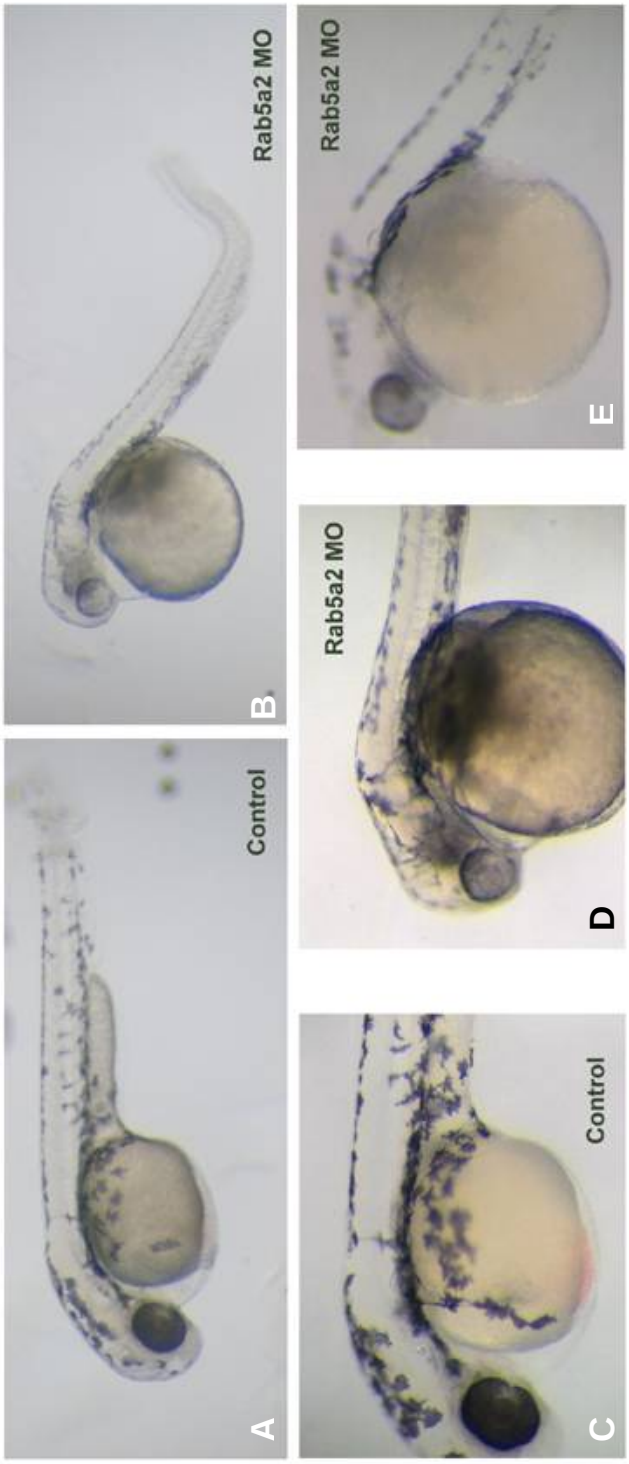

Figure 5.5.1: Lateral view of embryos injected with *rab5a2* MO at 1000 cell stage (B) compared to those injected with a control MO at 1000 cell stage (A). Magnified images of the head and yolk of embryos when injected with *rab5a2* MO at 1000 cell stage under reflected and direct lighting (D and E) compared to those injected with a control MO at 1000 cell stage (C).

5.5.2 Expression of β-catenin in rab5a2 MO injected embryos

β-Catenin localizes to the future dorsal side of the embryo early in development and is one of the earliest DV markers. The *rab5a2* MO injected embryos showed not only a lack of nodal target genes but also a lack of *cyc* expression. This suggested that, *rab5a2* may affect a factor upstream of nodal signalling. It is, therefore, possible that Rab5a2 may be involved in localization of β-Catenin. In order to investigate, this, control and *rab5a2* MO injected embryos were stained, using a β-Catenin antibody conjugated to biotin. The control embryos showed a gradient of staining emanating from the dorsal side of the embryo. Half of the *rab5a2* MO injected embryos showed no staining while three out of 12 of the embryos showed staining all over the embryos, the remainder were similar to controls (Figure 5.5.2).

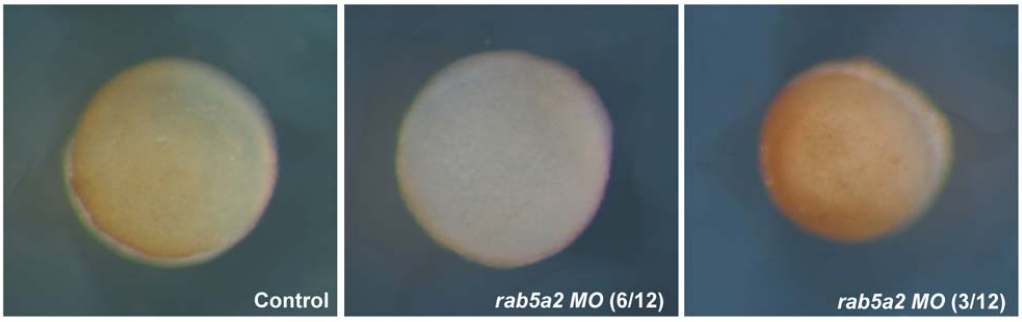

Figure 5.5.2: Animal view of *β-catenin* expression in control injected and *rab5a2* MO injected embryos at shield stage.